Traveling concentric-roll patterns in Rayleigh-Bénard convection with modulated rotation

Kim L. Thompson, Kapil M. S. Bajaj, and Guenter Ahlers
Department of Physics and iQuest, University of California, Santa Barbara, California 93106
(Received 10 October 2001; published 5 April 2002)

We present experimental results for pattern formation in Rayleigh-Bénard convection with modulated rotation about a vertical axis. The dimensionless rotation rate Ω was varied as $\Omega_m=\Omega[1+\delta\cos(\phi\Omega t)]$ (time is scaled by the vertical viscous diffusion time of the cell). We used a cylindrical cell of aspect ratio (radius/height) $\Gamma=11.8$ and varied Ω, δ, ϕ, and $\epsilon\equiv R/R_c(\Omega)-1$ (R is the Rayleigh number). The fluid was water with a Prandtl number of 4.5. Sufficiently far above onset even a small $\delta\gtrsim 0.02$ stabilized a concentric-roll (target) pattern. Multiarmed spirals were observed close to onset. The rolls of the target patterns traveled radially inward independent of the sense of rotation. The radial speed v was nearly independent of ϵ for fixed Ω, δ, and ϕ. However, v increased with any one of Ω, δ, and ϕ when all the other parameters were held fixed.

DOI: 10.1103/PhysRevE.65.046218 PACS number(s): 47.54.+r, 47.32.−y, 47.27.Te

Convection in a thin horizontal layer of fluid heated from below, known as Rayleigh-Bénard convection (RBC), presents a rich variety of phenomena when the control parameter is modulated. The usual control parameter is the Rayleigh number $R=\alpha g d^3\Delta T/\kappa\nu$, where α is the isobaric thermal expansion coefficient, g the vertical acceleration, ΔT the imposed temperature difference, and d the cell thickness. The fluid properties κ and ν are the thermal diffusivity and the kinematic viscosity. Without modulation convection begins when R exceeds a critical value $R_c(\Omega=0)$ which for the laterally infinite system has the value 1708 [1]. Modulation of ΔT [2–6] and of g [2,7] were explored in some detail and were found to shift the threshold and critical wave number and to produce interesting patterns above onset.

Here we report pattern-formation phenomena in the case of RBC with rotation about a vertical axis. In that case the frequency of rotation $\Omega=2\pi f\tau_\nu$, with f the frequency in Hz and $\tau_\nu=d^2/\nu$, is an additional control parameter. The usual equation of motion (in the rotating frame) acquires additional terms $2\Omega(\mathbf{v}\times\hat{\mathbf{z}})$ corresponding to the Coriolis force and $\Omega^2\hat{\mathbf{z}}\times(\hat{\mathbf{z}}\times\mathbf{r})$ corresponding to the centrifugal force. The centrifugal force, to lowest order, is balanced by a pressure gradient supported by the sidewalls, and its influence on the patterns is usually neglected. The Coriolis force leads to a threshold shift from $R_c(\Omega=0)$ to $R_c(\Omega)>R_c(0)$, to a change in the critical wave number $k_c(\Omega)>k_c(0)$, and to interesting pattern-formation phenomena. Perhaps most interesting are the patterns generated by the Küppers-Lortz (KL) instability [8] of the straight convection rolls which form above onset via a supercritical bifurcation. Immediately above onset the KL instability leads to a chaotically time dependent pattern of convection rolls which is broken up into domains of various orientations and which contains many dislocations [9,10].

In the present work Ω was modulated as

$$\Omega_m=\Omega[1+\delta\cos(\phi\Omega t)] \tag{1}$$

where the dimensionless time $t=\tilde{t}/\tau_\nu$ is scaled by τ_ν. This leads to an angular acceleration term $(\hat{\mathbf{z}}\times\mathbf{r})d\Omega/dt$ which induces an oscillating azimuthal mean flow (MF). Such a flow is expected to stabilize rolls with their axes parallel to its direction [11]. Recently, the problem was investigated theoretically by Roxin and Riecke [12], who found that the anisotropy imposed by the azimuthal MF tends to suppress the KL instability and to stabilize spirals and concentric rolls known as target patterns. In a model system, their detailed stability analysis allows a prediction of the number of spiral arms.

The parameter space for this problem is quite large and composed of the distance from threshold (without modulation) $\epsilon\equiv R/R_c(\Omega)-1$, the mean rotation rate Ω, the modulation amplitude δ, and the modulation frequency ϕ. In the present paper we explore only some of it, concentrating on properties of the target patterns.

Figure 1 shows typical patterns for $\Omega=23.6$ and $\epsilon\simeq 0.1$. For this Ω the unmodulated system is expected to be KL unstable [8]. Indeed, in the absence of modulation we observed a pattern typical of the KL state as shown in (a). Even a small modulation amplitude $\delta\gtrsim 0.02$ stabilized a target pattern as shown in (c). Not expected was the fact that this pattern traveled radially inward, causing rolls to disappear at the umbilicus. The traveling nature of the patterns is illustrated in Fig. 2, which shows the shadowgraph signal along a cell diameter as a function of time for several values of the modulation frequency ϕ. The direction of travel was independent of the sense of rotation. When ϕ was decreased or close enough to threshold for any ϕ, a pattern of multiarmed spirals appeared instead of the target patterns as shown in Fig. 1(b).

In the remainder of this paper we report measurements of

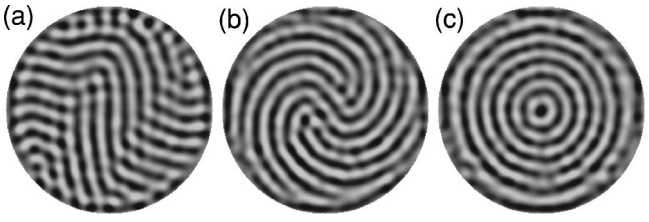

FIG. 1. Representative shadowgraph images just above onset in the absence and presence of modulation for $\Omega=23.6$ and $\epsilon\simeq 0.1$. (a) $\delta=0$, (b) $\delta=0.18$ and $\phi=1$, (c) $\delta=0.18$ and $\phi=5$.

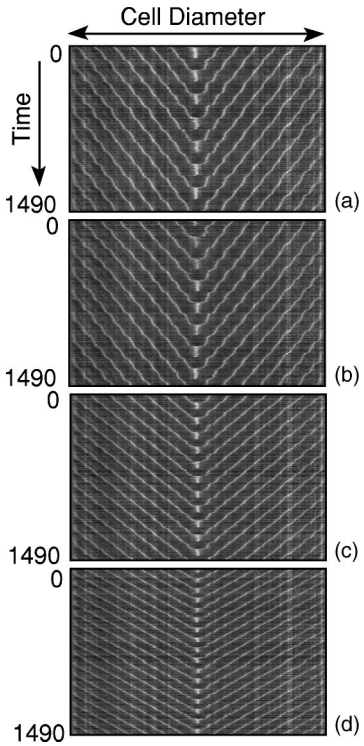

FIG. 2. Space-time plot of the radial shadowgraph signal as a function of time. The data are for $\Omega=19.7$, $\delta=0.18$, and $\epsilon=0.24$, and correspond to (a) $\phi=1$, (b) $\phi=2$, (c) $\phi=4$, and (d) $\phi=5$. The time is in units of τ_ν.

the radial speed v of the target patterns. With Ω, δ, and ϕ fixed, v was found to be almost independent of ϵ as shown in Fig. 3. Thus we studied in some detail the effects of Ω, δ, and ϕ on v by varying one of the parameters at a time.

The experiments were carried out in an apparatus described elsewhere [13]. We used a cylindrical cell made by sealing a high-density polyethylene ring between a 9.5 mm thick, optically flat sapphire top and a bottom silver plate of the same thickness, which had a diamond-machined top surface. The cell had a thickness $d=2.95\pm0.01$ mm with an

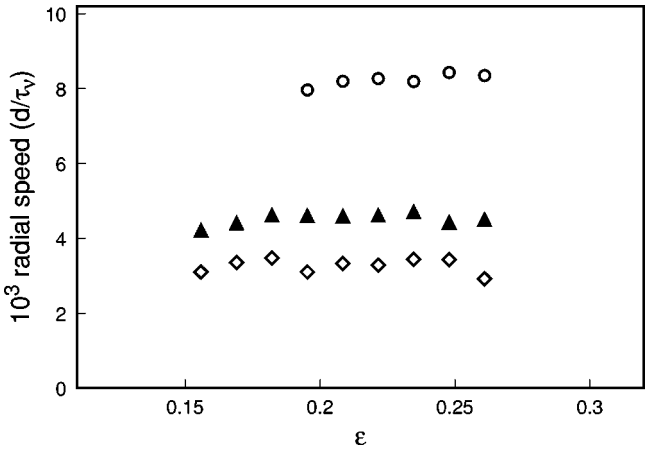

FIG. 3. Radial speed v as a function of ϵ for $\Omega=15.8$ and $\phi=1$. Open diamonds: $\delta=0.10$. Solid triangles: $\delta=0.15$. Open circles: $\delta=0.20$.

aspect ratio Γ ($\equiv$radius/d)$=11.8$. The working fluid was pure deionized water and was sealed in the cell with ethylene-propylene O rings. The top sapphire plate was in thermal contact with a constant-temperature circulating water bath at 37.0 °C. The experiments were carried out by varying the bottom-plate temperature near 40 °C. The Prandtl number of the working fluid was close to 4.5 for all the experiments. The vertical diffusion time τ_ν was 12.5 s and the characteristic velocity $v_\nu\equiv d/\tau_\nu$ was 236 μm/s. The Boussinesq parameter $\mathcal{P}$ [14,10] varied from -0.2 to -0.35. The whole apparatus was on top of a table that could be rotated at a maximum rate of 1 Hz. To limit the effects of centrifugal acceleration, the modulation experiments were carried out up to a rotation rate of only 0.35 Hz. The maximum value of the Froude number $F\equiv r(2\pi f)^2/g$, which measures the effect of the centrifugal acceleration, was only about 0.016 when $r=\Gamma d$ was used in its evaluation. With this setup, we were able to explore a modest range of rotation rates up to $\Omega\simeq28$. The modulation of rotation was achieved by varying the square-wave input of the controller of the stepper motor which drove the table. To ensure a smooth rotation, we built the modulation curve using 180 to 360 steps per revolution. We were able to explore the ranges $0\leqslant\epsilon\leqslant0.3$, $8\leqslant\Omega<28$, $0\leqslant\delta\leqslant0.24$, and $1\leqslant\phi\leqslant5$.

The onset of convection was determined both by heat-transport measurements and from the shadowgraph contrast. The critical temperature difference without rotation $\Delta T_c(\Omega=0)=1.92$ °C is in very good agreement with the estimate 1.927 ± 0.03 °C based on the fluid properties, $R_{c,0}=1708$, and the cell spacing. A pattern of straight rolls appeared just above the $\Omega=0$ onset. In the experiments with uniform rotation ($\Omega_m=\Omega$), the pattern was that of the expected S-shaped rolls at low Ω and the KL instability at higher Ω [9]. However, when the onset was approached from below in the presence of modulation, a pattern of multiarmed spirals appeared just above the onset in which rolls met the sidewalls at small angles [Fig. 1(b)]. The spirals, once formed, persisted for a significant range of ϵ above onset. Nonetheless, it was possible to create target patterns, and they were also stable over a significant range of ϵ when onset was approached from above in the presence of modulation. This could be achieved by starting below onset and applying a step in the heat current to the system while it was rotated at a uniform Ω. About 20% above the onset, a small modulation was turned on. This stabilized the existing concentric rolls that had appeard above onset due to dynamic sidewall forcing [15].

With modulation, the target patterns were not stationary but traveled inward as discussed above and illustrated in Fig. 2. The rings collapsed in the center of the cell as new ones were formed near the sidewall. This fascinating process went on indefinitely. To establish that the traveling target pattern was in fact due to modulation, we switched back to uniform rotation in several experiments. Cross rolls appeared at the periphery of the cell and eventually led to breaking up of the target pattern and the reappearance of KL-unstable roll patterns. The change of the pattern after modulation was turned off was accompanied by a slight decrease of the wave num-

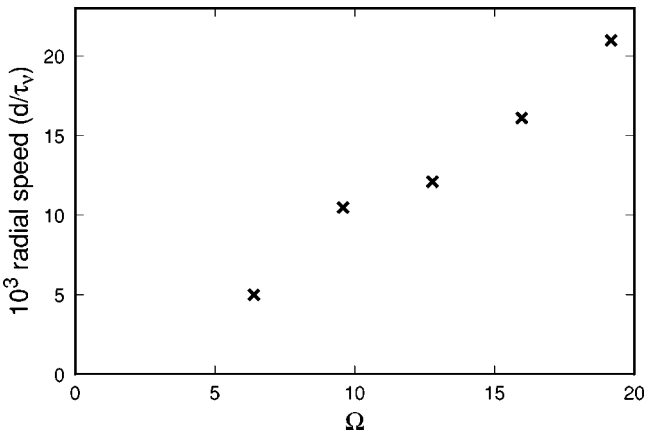

FIG. 4. Radial speed v as function of the mean rotation rate Ω for $\delta=0.18$, $\phi=5$, and $\epsilon=0.24$.

ber. The phenomena associated with switching off the modulation were quite interesting, but have not been studied in detail. Our focus was the appearance and dynamics of the target patterns. Since they could be stabilized only well above the onset, all of the experiments reported here were carried out by preparing the state by applying modulation when the bottom plate was being heated. All data reported were taken by approaching the onset from above. Just above the onset, the target pattern usually broke into spirals like those in Fig. 1(b).

First we examined the traveling-wave speed v of the target patterns as a function of ϵ at constant $\Omega=15.8$ and $\phi=1.0$ for three values of δ. Results are shown in Fig. 3. We see that v is nearly independent of ϵ. To explore the behavior of v as Ω is varied, several experiments were carried out in which a constant distance $\epsilon=0.24$ above onset was maintained at each Ω. Data for $\delta=0.18$ and $\phi=5$ are shown in Fig. 4. One sees that v increases with Ω at fixed δ and ϕ. A relatively high value $\delta=0.18$ and the largest $\phi=5$ were chosen for these measurements because the runs at small Ω, δ, and ϕ yielded a very weak shadowgraph signal which made it difficult to determine v. Also, at small $\delta<0.1$, although the target pattern was stable, the rolls traveled relatively slowly and it was difficult to measure v in a run of reasonable length.

Next we looked at the dependence of v on δ at fixed Ω and ϕ. This is shown in Fig. 5 for $\Omega=15.76$ and 7.9 and $\phi=1$. For $\Omega=7.9$ the pattern was stationary below $\delta=0.1$. Again for these sets of experiments $\epsilon=0.24$. Finally, in Fig. 6 results are shown for v as a function of ϕ at constant Ω, r, and δ. Although there is some ϕ dependence, the speed does not seem to go to zero as ϕ vanishes.

In this brief paper we reported on the effect of temporal modulation of the rotation rate on pattern formation in RBC in the presence of rotation about a vertical axis. In our parameter range we found that modulation generally produces spirals at onset. Further above onset target patterns can also be created, and once formed, they are stable to within several percent of the onset where they become unstable to spirals. The spirals or targets replace the Küppers-Lortz-unstable pattern or, at lower Ω, the S-shaped rolls that occur in the

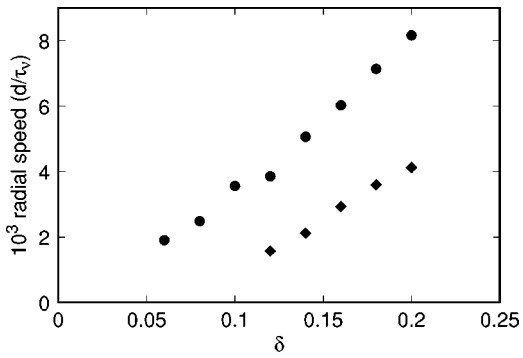

FIG. 5. Radial speed v as function of the amplitude of modulation δ for two different Ω and $\phi=1$. Solid circles: $\Omega=15.8$ and $\epsilon=0.24$. Diamonds: $\Omega=7.9$ and $\epsilon=0.24$.

absence of rotation. We found that the concentric rolls of the target patterns travel inwardly and disappear at the umbilicus, with new ones being generated at the sidewall. The direction of travel is independent of the direction of rotation. We report quantitative measurements of the traveling-wave speed as a function of the Rayleigh number, the average rotation rate, the modulation amplitude, and the modulation frequency.

It is not difficult to understand the stabilization of spirals or targets. The angular acceleration is expected to induce an oscillating azimuthal mean flow. A mean flow is known to stabilize convection rolls with their axes in the direction of the flow [11], and thus its azimuthal nature in the present case quite naturally leads to targets or (for relatively weak flow) to spirals. This phenomenon is discussed more quantitatively in an accompanying paper by Roxin and Riecke [12]. It is more difficult to understand the traveling nature of the rolls in the target patterns, and we are not aware of a theoretical explanation. A conceivable cause of the roll drift may be the *radial* large-scale flow induced by the centrifugal force. Although we cannot rule this out on the basis of the present experiments, it seems an unlikely explanation to us because of the quite small Froude numbers involved in our work. We also note that this flow differs from the usual mean flow that is known to induce roll drift in that it has no vertical vorticity; i.e., its direction of motion is in opposite directions near the top and the bottom of the fluid layer. Thus at lowest order it would not be expected to induce roll drift.

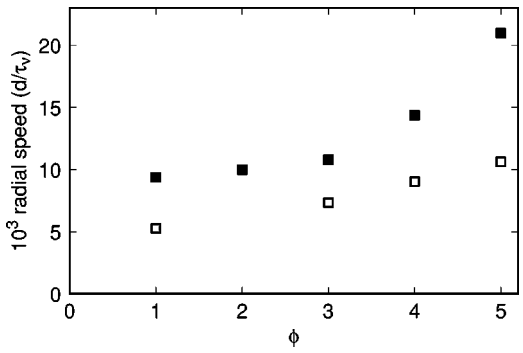

FIG. 6. Radial speed v as function of ϕ for $\Omega=19.7$ (solid squares) and 11.8 (open squares), $\epsilon=0.24$, and $\delta=0.18$.

More experiments to clarify this point, involving a study of the roll velocity as a function of the Froude number, would be appropriate. Alternatively, it has been suggested that the Coriolis force due to the azimuthal mean flow may play a role [16]. This effect would have to be quite subtle since the major component of this force oscillates and alternately points radially outward and inward during each modulation cycle. At present this possibility has not yet been investigated theoretically. Thirdly, an interesting possibility is that competing wave-number-selection mechanisms at the umbilicus and at the sidewall become relevant in the presence of modulation. Such a competition would lead to a radial wave number gradient and thus to a mean drift of the rolls in a direction orthogonal to their axes [17]. The occurrence of this phenomenon due to highly conducting sidewalls was investigated theoretically by Tuckerman and Barkley [18]. For $\Omega=0$ [19,20] (and indeed for $\Omega>0$ but $\delta=0$ [21]) it does not seem to occur in experiments, presumably because the sidewalls pin the phase of the pattern. A modification of the sidewall selection and/or a reduction of the phase pinning by the modulation would be an interesting topic for future theoretical study. Experimental support for drift due to a wave number gradient could be found from measurements in cells with different aspect ratios, since v would be proportional to $1/\Gamma$. Of course, an actual measurement of the radial dependence of the local wave number would be very interesting as well, but was beyond the resolution of the current experiments.

We are grateful to Lorenz Kramer, Werner Pesch, Hermann Riecke, and Alex Roxin for stimulating discussions. This work was supported by the U.S. Department of Energy through Grant No. DE-FG03-87ER13738. One of us (G.A.) is thankful for support by NATO Linkage Grant No. CRG.LG.973103.

[1] S. Chandrasekhar, *Hydrodynamic and Hydromagnetic Stability* (Oxford University Press, London, 1961).
[2] G. Ahlers, P. C. Hohenberg, and M. Lücke, Phys. Rev. A **32**, 3493 (1985); **32**, 3519 (1985), and references therein.
[3] C. W. Meyer, D. S. Cannell, G. Ahlers, J. B. Swift, and P. C. Hohenberg, Phys. Rev. Lett. **61**, 947 (1988).
[4] J. K. Bhattacharjee, J. Phys. A **22**, L1135 (1989); Phys. Rev. A **41**, 5491 (1990).
[5] J. J. Niemela, M. R. Smith, and R. J. Donnelly, Phys. Rev. A **44**, 8406 (1991).
[6] C. Meyer, D. S. Cannell, and G. Ahlers, Phys. Rev. A **45**, 8583 (1992).
[7] J. L. Rogers, M. F. Schatz, J. L. Bougie, and J. S. Swift, Phys. Rev. Lett. **84**, 87 (2000); J. L. Rogers, M. F. Schatz, O. Brausch, and W. Pesch, *ibid.* **85**, 4281 (2000).
[8] G. Küppers and D. Lortz, J. Fluid Mech. **35**, 609 (1969); G. Küppers, Phys. Lett. **32A**, 7 (1970); R. M. Clever and F. H. Busse, J. Fluid Mech. **94**, 609 (1979).
[9] Y. Hu, W. Pesch, G. Ahlers, and R. E. Ecke, Phys. Rev. E **58**, 5821 (1998); and references therein.
[10] For a recent review, see E. Bodenschatz, W. Pesch, and G. Ahlers, Annu. Rev. Fluid Mech. **32**, 709 (2000).
[11] See, for instance, R. M. Clever and F. H. Busse, J. Fluid Mech. **229**, 517 (1991); R. E. Kelly, Adv. Appl. Math. **31**, 35 (1994), and references therein.
[12] A. Roxin and H. Riecke, following paper, Phys. Rev. E **65**, 046219 (2002).
[13] G. Ahlers, D. S. Cannell, L. I. Berge, and S. Sakurai, Phys. Rev. E **49**, 545 (1994).
[14] F. H. Busse, J. Fluid Mech. **30**, 625 (1967).
[15] See, for instance, G. Ahlers, M. C. Cross, P. C. Hohenberg, and S. Safran, J. Fluid Mech. **110**, 297 (1981); M. Cross, P. Hohenberg, and M. Lücke, *ibid.* **136**, 169 (1983).
[16] W. Pesch (private communication).
[17] See, for instance, I. Rehberg, E. Bodenschatz, B. Winkler, and F. H. Busse, Phys. Rev. Lett. **59**, 282 (1987).
[18] L. S. Tuckerman and D. Barkley, Phys. Rev. Lett. **61**, 408 (1988).
[19] E. L. Koschmieder and S. G. Pallas, Int. J. Heat Mass Transf. **17**, 991 (1974).
[20] Y. Hu, R. Ecke, and G. Ahlers, Phys. Rev. E **48**, 4399 (1993).
[21] Y. Hu, R. E. Ecke, and G. Ahlers, Phys. Rev. E **55**, 6928 (1997).